Emergent topological excitations in a two-dimensional quantum spin system

Hui Shao,[1] Wenan Guo,[1,2,*] and Anders W. Sandvik[3,†]

[1]*Department of Physics, Beijing Normal University, Beijing 100875, China*
[2]*State Key Laboratory of Theoretical Physics, Institute of Theoretical Physics, Chinese Academy of Sciences, Beijing 100190, China*
[3]*Department of Physics, Boston University, 590 Commonwealth Avenue, Boston, Massachusetts 02215, USA*

We study the mechanism of decay of a topological (winding-number) excitation due to finite-size effects in a two-dimensional valence-bond solid state, realized in an $S = 1/2$ spin model ($J - Q$ model) with six-spin interactions and studied using projector Monte Carlo simulations in the valence bond basis. A topological excitation with winding number $|W| > 0$ contains domain walls, which are unstable due to the emergence of long valence bonds in the wave function, unlike in effective descriptions with the quantum dimer model (which by construction includes only short bonds). We find that the lifetime of the winding number in imaginary time, which is directly accessible in the simulations, diverges as a power of the system length L. The energy can be computed within this time (i.e., it converges toward a "quasieigenvalue" before the winding number decays) and agrees for large L with the domain-wall energy computed in an open lattice with boundary modifications enforcing a domain wall. Constructing a simplified two-state model which can be solved in real and imaginary time, and using the imaginary-time behavior from the simulations as input, we find that the real-time decay rate out of the initial winding sector is exponentially small in L. Thus, the winding number rapidly becomes a well-defined conserved quantum number for large systems, supporting the conclusions reached by computing the energy quasieigenvalues. Including Heisenberg exchange interactions which bring the system to a quantum-critical point separating the valence-bond solid from an antiferromagnetic ground state (the putative "deconfined" quantum-critical point), we can also converge the domain-wall energy here and find that it decays as a power law of the system size. Thus, the winding number is an emergent quantum number also at the critical point, with all winding number sectors becoming degenerate in the thermodynamic limit. This supports the description of the critical point in terms of a U(1) gauge-field theory.

I. INTRODUCTION

Systems with topological order are characterized by unconventional quantum numbers labeling degenerate ground states, the number of which depends on boundary conditions. Except for models where conservation of topological numbers is ensured by construction, such as Kitaev's toric code [1,2], in general a topological quantum number is only emergent in the limit of infinite system size. For a finite system the lifetime of a state prepared with a fixed topological number is finite, and, thus, the levels within the ground-state manifold are split. One would normally expect the lifetime to be exponentially long in the system size, as in the case of an ordered state with a broken discrete symmetry (e.g., an Ising ferromagnet in a weak transverse field). In practice, e.g., when considering the design of topologically protected qubits [3–6], the lifetime due to finite system size then may not play an important role if the qubit is sufficiently large. It is still useful to investigate quantitatively the mechanism of these instabilities due to finite size in various topological states. The emergence of topological conservation laws is also of interest in descriptions of quantum matter using simplified Hamiltonians and quantum field theories where they are conserved by construction, e.g., in dimer models and field theories derived from them [7,8].

Topological quantum numbers are often discussed in the context of quantum spin liquids [9–12] but can also appear in systems with long-range order. Here we investigate a quantum

spin $S = 1/2$ Hamiltonian which has a valence bond (VB) ordered (spontaneously dimerized) ground state and whose excitations containing domain walls can be classified by a winding number (which essentially counts the number of domain walls in the system). In this case the ground state of a large system is in one winding number sector and the other sectors are at higher energy. Our interest here is to study quantitatively the instabilities of the domain walls and the topological mechanisms (changes of the winding number) responsible for their decay in finite systems. This issue is of particular interest when the VB solid order is weakened by the introduction of interactions that eventually completely destroy the order and bring about other phases. In this process the winding numbers should also become unstable in the thermodynamic limit. In our studies discussed here, we use the so-called $J - Q$ model on the square lattice [13,14], where J is the standard antiferromagnetic Heisenberg exchange and Q a multispin (here six-spin) interactions favoring VB order.

The singlet sector of the SU(2) invariant spin system considered here is amenable to a description in the VB basis [15–18], where a state of an even number of spins N is a superposition of product states containing $N/2$ singlet pairs (VBs), for which we use the notation

$$(a,b) = (\uparrow_a \downarrow_b - \downarrow_a \uparrow_b)/\sqrt{2}. \tag{1}$$

While the winding number is strictly conserved within a restricted basis of short VBs (bond lengths $< L/4$, where L is the system length, as we will explain in detail below) [19], with all bond lengths included, as required for the basis to be complete (whence the basis in fact becomes overcomplete),

---
*waguo@bnu.edu.cn
†sandvik@bu.edu

the winding number is no longer conserved, and, thus, domain walls can decay due to topological fluctuations. We here study such decay within the imaginary-time dynamics accessible in projector quantum Monte Carlo (PQMC) simulations in the VB basis [20,21].

We find that an initial state with domain walls decays to the ground state with no domain walls through transitional states with a high density of long VBs. As a result, the lifetime is only growing with the system size as a power law. The analytic continuation between imaginary and real time is very complex for the nonequilibrium situation considered here, and we cannot translate the imaginary-time behavior rigorously to real-time evolution, where an isolated system should thermalize at constant energy instead of decaying to the ground state. To gain some insights into the relevant real-time scale corresponding to the power-law divergent imaginary-time scale of the winding number, we consider an effective two-state model in combination with the PQMC data. Based on this approximation an exponentially long lifetime in real time appears plausible, both in the VB solid phase and at the critical point separating it from an antiferromagnetic ground state.

In addition to the lifetime of the winding number, we also discuss the quasieigenenergies of the winding states in the VB solid and at the critical point. Comparisons with domain-wall calculations in boundary-modified systems with forced domains confirm the domain-wall nature of the states with nonzero winding number.

In Sec. II we will discuss the winding number in detail and explain our methods to investigate its fluctuations in PQMC simulations. Results of such simulations in the VB solid phase of the $J - Q$ model are presented in Sec. III. In Sec. IV we introduce the effective two-state model and study the relationship between imaginary-time decay to the ground state and transition rates in real time. We consider scaling in a quantum-critical system and the eventual instability of the winding number sectors in the antiferromagnetic phase in Sec. V. In Sec. VI we summarize and further discuss our results and their implications.

II. DIMERS, VALENCE BONDS, AND WINDING NUMBERS

To more precisely introduce the concepts and mechanisms to be discussed below, consider first the winding number $W = (w_x, w_y)$ of a classical close-packed dimer model on the square lattice. A dimer connects two nearest-neighbor sites, one on sublattice A and one on B, with the A and B sites forming a checkerboard pattern. W can be defined by assigning a direction (arrow) A $\rightarrow$ B for each dimer. Superimposing any such configuration onto a reference configuration with $B \rightarrow A$ dimers forming (by convention) horizontal columns, closed loops form and w_x, w_y correspond to the x and y currents normalized by the system length L.

The classical dimer configurations are the basis states of the quantum dimer model (QDM) [22–24], which in the simplest case has a diagonal term counting the number of pairs of parallel bonds and an off-diagonal term which can rotate such "flippable pairs" by 90°. The off-diagonal terms being local, they cannot change W, which, thus, is a good quantum number of the QDM on a periodic lattice. The Hilbert space consists of

$\sim L^2$ winding number sectors. On a nonbipartite lattice, e.g., the triangular lattice, or in an extended square-lattice model including also bonds connecting next-nearest neighbors [25], some winding numbers mix and the sectors are reduced down to even and odd ones [19,26], labeled, e.g., by $w_x, w_y = \pm 1$. On the torus there are thus four sectors of conserved W.

Now consider $S = 1/2$ spins. Any total spin singlet can be written as a superposition of tilings with VBs, and if the system is bipartite one can restrict the bonds to only connect sites on different sublattices. If the subscripts a and b in Eq. (1) correspond to the sublattices as $a \in A, b \in B$, the sign of each component of $|v\rangle = |(a_1, b_1) \cdots (a_{N/2}, b_{N/2})\rangle$ in the $\uparrow, \downarrow$ basis conforms with Marshall's sign rule for the ground state of a bipartite system. Such a state can be expanded in VB states,

$$|\Psi_0\rangle = \sum_v f_v |v\rangle, \qquad (2)$$

with positive-definite expansion coefficients f_v (where v labels the bond configurations, $v \in \{1, \ldots, (N/2)!\}$, which map into permutations of the $N/2$ A sites connected to $N/2$ B sites) [16,17]. The VB basis states are nonorthogonal, with $\langle v_2 | v_1 \rangle = 2^{n_{12} - N/2}$, n_{12} being the number of loops in the transition graph of the VB configurations [16,17].

The insight that many quantum states of spins can, to a good approximation, be expressed with short VBs motivated the introduction of the QDM as a class of effective models to describe some quantum spin systems, spin liquids in particular [22–24,27–30]. To judge whether the QDM indeed provides a good description in a given case, one has to consider the role of long bonds, the nonorthogonality of the VB basis, and the interactions included in the QDM (for which there is a systematic scheme [31,32]). In general it is not possible to rigorously prove the validity of the QDM description other than by careful comparisons of numerical results when available.

The QDM should provide an excellent approximation for a VB solid (crystal), where predominantly short VBs form a regular density pattern. Such ground states are hosted by many quantum spin models with frustrated exchange interactions in parts of their parameter spaces [33–37], and also by models with certain multispin couplings beyond the pair exchange [13,14,38,39]. One of the latter is the $J - Q$ model [13], where J is the antiferromagnetic Heisenberg exchange, which we can write as

$$H_J = -J \sum_{b=1}^{2N} P_{i(b)j(b)}, \qquad (3)$$

where P_{ij} is a singlet projector,

$$P_{ij} = (1/4 - \mathbf{S}_i \cdot \mathbf{S}_j), \qquad (4)$$

and b labels the links connecting nearest neighbors $i(b), j(b)$ on the square lattice with $N = L^2$ sites. For the Q term we use the six-spin variant [14],

$$H_Q = -Q \sum_{c=1}^{2N} P_{i(c)j(c)} P_{k(c)l(c)} P_{m(c)n(c)}, \qquad (5)$$

where the cells c contain three nearest-neighbor site pairs $(ij)(kl)(mn)$ forming 2×3 and 3×2 plaquettes. The model $H(J, Q) = H_J + H_Q$ has a strongly ordered columnar VB

solid ground state for large Q/J [40]. We will here first study $H = H_Q$ as a stand-alone model [40] and later tune Q/J to the critical point at which the VB solid order vanishes and antiferromagnetic order sets in.

Performing PQMC simulations in the overcomplete bipartite VB basis, we have access to the winding number and our aim is to study its stability as a function of the system size. A columnar arrangement of short VBs has winding number $W = (0,0)$ and any other W corresponds to the presence of domain walls, as illustrated in Fig. 1. Domain walls have been studied within QDMs [8], including quantum phase transitions driven by increasing winding number (density of domain walls) [7]. Here our motivation differs, but it is useful to have a VB solid of the QDM as a reference point, where the winding numbers characterizing states with domain walls are fully conserved by construction.

In this study we use the imaginary-time Schrödinger evolution operator

$$U(\tau) = e^{-\tau H}, \qquad (6)$$

and apply it in PQMC simulations [41] to an initial state $|\Psi_0(w_x)\rangle$ with only short (nearest-neighbor) bonds and winding number $(w_x, 0)$. A $w_x \neq 0$ state is obtained from a perfect columnar state by shifting an odd number of rows, as illustrated in Fig. 1 for $w_x = 1$. We have $U(\tau \to \infty)|\Psi_0(w_x)\rangle \to |0\rangle$ (neglecting an unimportant normalization), where $|0\rangle$ is the ground state, which is dominated by the $w_x = 0$ sector; for $L \to \infty$ the probabilities approach $P(w_x = 0) = 1$ and $P(w_x = 1) = 0$ exponentially with increasing L.

In the program implementation of the above PQMC approach, we Taylor expand the operator (6) to all contributing orders, as in the stochastic series expansion (SSE) method [42,43]. Thus, each configuration consists of a series of $n \propto N\tau$ operators which are sampled from the two- and six-spin terms in Eqs. (3) and (5). In the model with $J = 0$ and $Q = 1$ that we will study first, there is, thus, a total of $3n$ singlet projectors acting on the initial state for a term of order n, while with both $J > 0$ and $Q > 0$ there are both two- and six-spin operators present and the total number of singlet projectors is between n and $3n$.

To see how the presence of long bonds leads to nonconservation of W we discuss a one-dimensional example with eight spins, illustrated in Fig. 2. The reference configuration used to define $W \in \{0,1\}$, which by definition itself has $W = 0$, is shown in Fig. 2(a), while Fig. 2(b) shows its transition

FIG. 2. (Color online) Illustration of the winding number and its nonconserved property for an eight-site chain. The open and solid circles indicate sublattices A and B, respectively, and the lines and arcs with arrows are the VBs. In (a) the reference configuration for defining W is shown, and in (b) it has been superimposed with a state with $W = 1$. In (c) a singlet projector has acted on the $W = 1$ state, at sites 3 and 4 from the left, and in (d) a subsequent action on sites 5 and 6 has lead to a change of the winding number to $W = 0$ (the bonds lost in the processes are shown with dashes).

graph with the $W = 1$ short-bond state. In Fig. 2(c) a singlet projector has acted on the $W = 1$ state and reconfigured two bonds, leading to a new bond of length 1 and one of length 3. The winding number remains at $W = 1$. A second operation in Fig. 2(d) leads to a bond which in a longer chain would have length 5, but in this $L = 8$ periodic system has length $L - 5 = 3$ by definition of the VB basis. Then the winding number changes to $W = 0$. This is also in accord with an examination of the bond pattern, which now has the short bonds shifted by one lattice spacing relative to those in the original bond configuration. Quite generally, if the two bonds affected by a singlet projection span more than half the system length, then the winding number changes in the process, i.e., the minimum bond length required for W to not be conserved is $L/4$ for L being a multiple of 4. We study also L given by an odd multiple of 2, for which there are only small, trivial differences from the above in how the winding numbers change.

III. RESULTS IN THE STRONGLY ORDERED VALENCE-BOND SOLID STATE

If the winding number is conserved for $L \to \infty$, which we expect, then in this limit the projected state $U(\tau)|\Psi_0(w_x)\rangle$ should evolve toward the lowest eigenstate with winding number w_x. For finite L, one can expect there to be a "quasieigenstate" toward which the state evolves before w_x typically decays to lower values (with some fluctuations possible also to higher w_x) and the ground state is obtained. Sampling the norm $\langle \Psi_0(w_x)|U(\tau)U(\tau)|\Psi_0(w_x)\rangle$, we can use the estimator $\langle H \rangle = -\langle n \rangle/(2\tau)$, in analogy with the SSE method [42,43]. We classify a PQMC configuration as having a conserved winding number if propagation with U^2 from both the left and the right maintains w_x in its initial sector after each step. This way, we can compute the energy in different sectors and in the ground state for large-enough τ. We have reported preliminary results for the domain-wall energies in different winding sectors based on a slightly different procedure [44,45].
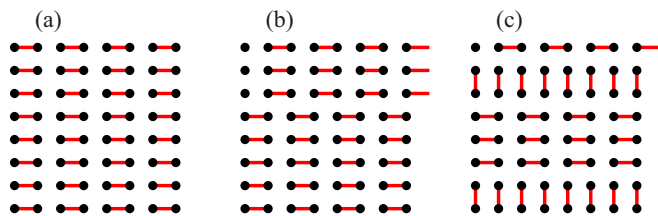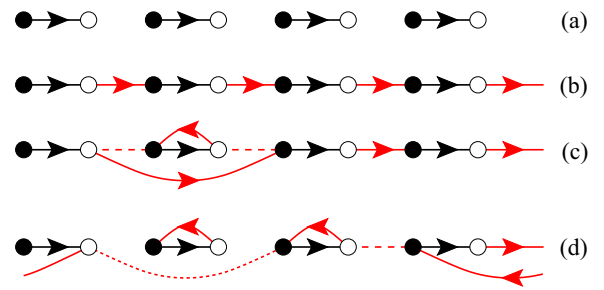

FIG. 1. (Color online) VB configurations with winding number $(0,0)$ in (a) and $(1,0)$ in (b) and (c), with (c) obtained from (b) by locally rotating pairs of dimers. Configuration (a) serves as the reference configuration for defining the winding numbers. These VB states are all used as initial states in the PQMC simulations discussed in this paper.
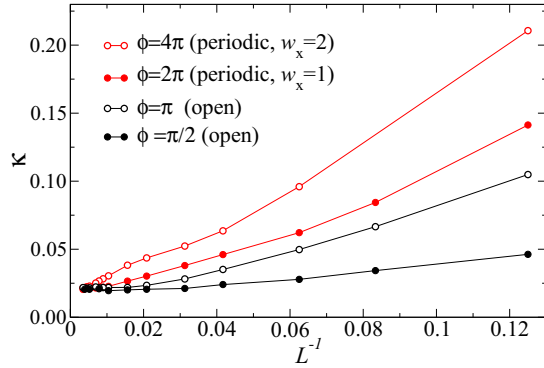
FIG. 3. (Color online) Domain-wall energies per unit length, normalized to a single domain wall with twist angle $\phi = \pi/2$. Results are shown for periodic systems in the sectors $w_x = 1, 2$ and for systems with open-boundary modifications enforcing domain walls. For the periodic systems the projection time was $\tau = L/8$. The angle ϕ indicated is the total twist of the VB order parameter when going around a periodic system or across an open system.

In Fig. 3 we show results for the quantity

$$\kappa(w_x, L) = \frac{\langle H \rangle_{w_x} - \langle H \rangle_0}{4L w_x}, \tag{7}$$

which can be interpreted as a domain-wall energy per unit length when converged. We previously computed the domain-wall energy based on systems with edge modifications favoring VB ordering in such a way that a single domain wall of the type in Fig. 1(b) is present or absent [44]. Such a domain wall can be classified as having a twist angle $\phi = \pi$ [40,46], while a domain wall between horizontal and vertical VB solids, as in in Fig. 1(c), has $\phi = \pi/2$ (and the π wall of course consists of two separate $\pi/2$ walls). In periodic systems the total VB twist angle is $2\pi w_x$. For the open systems we therefore define κ corresponding to Eq. (7) by dividing the energy difference of systems with and without domain walls by $2L\phi/\pi$. As can be seen in Fig. 3, the results of different calculations give consistent results for κ when for $L \rightarrow \infty$, confirming the above arguments.

Simulations for large periodic systems suffer from ergodicity problems (long equilibration times) due to which the system may stay for a very long time in the initial w_x sector, even at projection times τ where $w_x = 0$ should dominate (as judged by the behavior for smaller systems). In the energy calculation this is an advantage, as it allows us to converge very well to the $w_x \neq 0$ lowest quasieigenstates, in a way similar to measuring the energy of a metastable state in classical Monte Carlo simulations. Using $\tau = L/8$ and an initial state with $w_x = 1$, the calculations for L up to 32 in Fig. 3 showed fluctuating w_x, while runs for larger L typically stayed locked at $w_x = 1$.

The imaginary-time lifetime of the state evolved from $|\Psi_0(w_x)\rangle$ can be defined, e.g., as the τ at which the probability of remaining in the initial w_x sector is $1/2$. However, because of the aforementioned ergodicity problems this definition is practically useful only for relatively small system sizes. We have therefore developed an alternative approach, by using a long total projection time $\beta = M\Delta_\tau$, writing $U(\beta)$ as $U^M(\Delta_\tau)$, and individually Taylor-expanding each of these factors in the PQMC simulations. Then we can monitor the winding number

in the state propagated from the left and from the right with the full operator string (i.e., the concatenation of the M individual strings) and in both cases there will be some time "slice" $\tau = i\Delta_\tau$ (with i counted from the bra or ket initial state) at which the winding number changes from, say, $w_x = 1$ to 0. Once a system has equilibrated and β is large enough (so the energy has converged), we can measure the probability of staying in the initial w_x sector as a function of τ. This method has much less severe autocorrelation problems once a decay to $w_x = 0$ somewhere in the time space has occurred.

Some typical results for $w_x = 1$ are shown in Fig. 4, and the resulting lifetime $\tau_{1/2}(L)$, defined as the τ for which the probability $P(w_x = 1)$ of the state to stay in the initial sector equals $1/2$, is graphed in Fig. 5. While this definition of
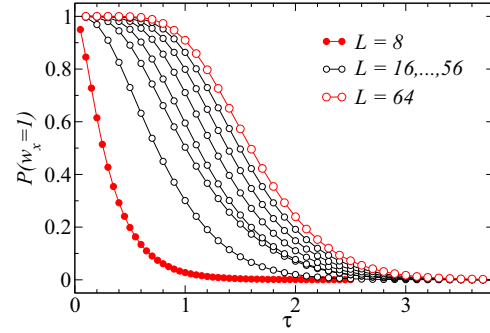

FIG. 4. (Color online) The probability of a state projected out of an initial state with $w_x = 1$ to remain in that winding number sector at time τ.
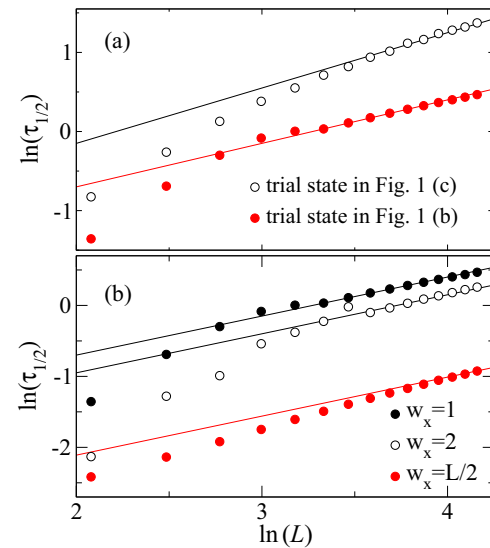

FIG. 5. (Color online) Lifetime, defined as the projection time $\tau = \tau_{1/2}$ at which $P(w_x) = 1/2$ (based on interpolation of data such as those in Fig. 4), versus the system size on a log-log scale. Panel (a) shows the behavior for $w_x = 1$ with two different initial states; generalizations of those depicted in Figs. 1(b) and 1(c). The lines show the forms $\sim L^{0.55}$ and $\sim L^{0.7}$ drawn through the large-L data obtained with initial states Figs. 1(b) and 1(c), respectively. In (b) the lifetimes for $w_x = 1, 2$ and $L/2$ are shown [using initial states of type Fig. 1(b)], along with the form $\sim L^{0.55}$ drawn through the large-L data.

$\tau_{1/2}$ is not, strictly speaking, based on a *bona fide* quantum mechanical expectation value, it nevertheless gives a lifetime of the same order as the original definition proposed earlier (and this can also be expected based on formal considerations of the dynamics generated by operator products [47]). For the system sizes where we have data available from both approaches, the original definition gives a somewhat larger value but similar size dependence. As seen in Fig. 5(a), after a crossover behavior for small L, the lifetime grows asymptotically as a power law L^{α}.

While the power-law behavior appears to be robust to variations in the initial state, the value of the exponent may not be. Using two different initial states of the types (b) and (c) depicted in Fig. 1, two different exponents α are obtained. The initial states both have $w_x = 1$, but (c) explicitly implements $\pi/2$ domain walls, while the state in (b) has sharp π domain walls. The π domain walls will split up into $\pi/2$ domain walls in the course of imaginary-time projection, and by implementing them from the outset the initial state is closer to the eventual $w_x = 1$ quasieigenstate. The range of system sizes for which the power law can be approximately fitted in Fig. 5(a) is rather small, and the exponents may still drift for larger systems. We can therefore not exclude that the exponents are asymptotically the same, though it also appears reasonable that state (b) is shorter-lived by a power of L, due to it being further away from the quasieigenstate because of the wrong kind of initial doman walls imposed.

In Fig. 5(b) we compare results for $w_x = 1$, $w_x = 2$, and the extreme case of $w_x = L/2$. In all cases the initial state was of the type in Fig. 1(b), with only horizontal bonds shifted to achieve the different winding numbers. The lifetime for $w_x > 1$ is also defined based on results such as those in Fig. 4, as the probability of still remaining in the original winding sector being $1/2$. The initial event of decay is almost always into a state with w_x one unit smaller than the initial value. In Fig. 5(b) we have fitted the results for all w_x and large L to the same power law $L^{0.55}$, though, again, there are considerable uncertainties in the exponents and we cannot conclude positively that they really are the same in all cases. The prefactor of the power law decreases with increasing w_x, but, interestingly, even for $w_x = L/2$ it is not that much smaller than at $w_x = 1$.
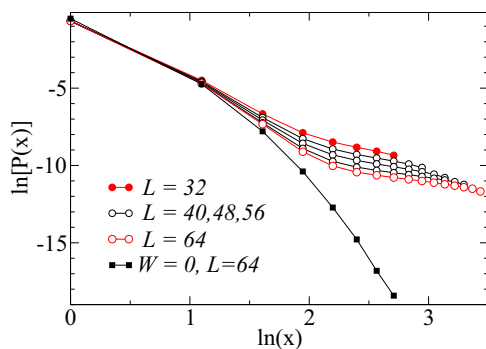

FIG. 6. (Color online) Bond-length probability for bonds of shape $(x,0)$ at projection time $\tau = \tau_{1/2}$ for different system sizes when the starting state has winding number $w_x = 1$ [of the type of the simple domain-wall state depicted in Fig. 1(b)]. For reference, results are also shown for the VB solid ground state ($W = 0$ sector).
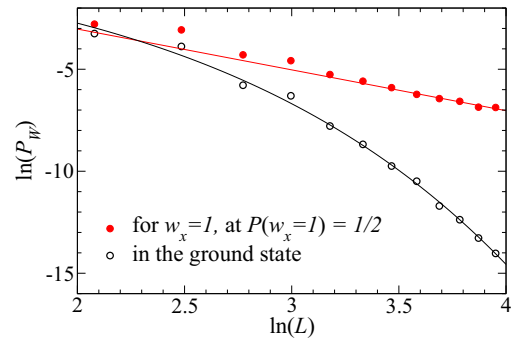

FIG. 7. (Color online) Log-log plot of the total probability of VBs of length $\geqslant L/4$ in the ground state and in the transient $w_x = 1$ states at $\tau_{1/2}$ versus the system size, obtained under the same conditions as the results in Fig. 6. The (red) straight line has slope -2, while the curve (black) shows the form $P_W \propto \exp(-aL^b)$ with $b \approx 0.7$.

With only short VBs the lifetime as defined above would be infinite. With the probability of long bonds decaying exponentially with the bond length in both the initial and final states (which we have confirmed), one might naively have expected an exponentially long lifetime. The reason for the much shorter lifetime is that long bonds are generated in the transient states through which the system evolves. Figure 6 shows the bond-length distribution for bonds of "shape" $(x,0)$ in the simulations with the initial state of type Fig. 1(b) at the point (in Fig. 4) where the probability $P(w_x = 1) = 1/2$. The results are compared to those in the VB solid ground state without domain walls.

Clearly, the transient state with the decaying domain walls has a dramatically larger fraction of long bonds, which suggests a way to understand the short lifetime: The projected state evolves toward the ground state through transitional states that have a very high fraction of long bonds relative to the ground state dominated by very short bonds. Note that the initial state we are using only has short bonds, and by looking at the metastable domain-wall quasieigenstate we also find that it is dominated by short bonds, very similar to the ground state. Our results show the presence of excited states which differ markedly and which can be components of the initial state (which they have to be in order to appear as a result of the PQMC procedure), at least in part because of the overcompleteness and nonorthogonality of the VB basis. The total fraction of bonds longer than $L/4$, i.e., those that can generate changes in the winding number, is graphed versus the system size in Fig. 7. It decays as L^{-2} in the case considered, while the decay is exponential in the ground state.

IV. EFFECTIVE TWO-STATE MODEL AND REAL-TIME EVOLUTION

It is not easy to relate our findings above to real-time evolution, where an isolated system would not decay to its ground state but go through a thermalization process with conserved excess energy density $\propto 1/L$. Also in this case one can define a time scale on which states with winding numbers that differ from the initial one become populated. In principle, our $\tau_{1/2}$ computed in the previous section should in some way

(through analytic continuation) be related to this time scale. While in some cases how to relate real and imaginary-time evolution is understood [48], in the present case there is no known way to do this based on numerical imaginary-time data.

To gain some insights into the real-time dynamics corresponding to the power-law increase in the imaginary lifetime with L, we consider an approximate but illuminating simple effective two-state model. We consider unperturbed states $|\downarrow\rangle$ and $|\uparrow\rangle$ corresponding to the $w_x = 0, 1$ sectors of the VB solid for large L, with energies $E_\downarrow = -\epsilon$ and $E_\uparrow = \epsilon$. To mimic the decay of a state initially in the higher-energy $w_x = 1$ sector to $w_x = 0$, we consider a perturbation by an off-diagonal matrix element $x \ll \epsilon$, i.e., the effective Hamiltonian

$$H_2 = \begin{pmatrix} -\epsilon & x \\ x & \epsilon \end{pmatrix}. \tag{8}$$

Starting with the initial state $|\psi(\tau)\rangle = |\uparrow\rangle$ we compute the probability $P(\uparrow) = |\langle\uparrow|\psi(\tau)\rangle|^2$ of the system staying in this initial state after time evolution using $U(\tau)$ in Eq. (6). Defining the lifetime by $P = 1/2$ as in the preceding section gives the exact result

$$e^{-2\tau\sqrt{\epsilon^2+x^2}} = \frac{r\sqrt{1+r^2} - r^2}{\sqrt{1+r^2}+1}, \tag{9}$$

where $r = x/\epsilon$. To leading order in r this becomes

$$e^{-2\tau\epsilon} = \frac{x}{2\epsilon}. \tag{10}$$

Using the scaling behaviors found using the PQMC simulations, $\epsilon \sim L$ and $\tau_{1/2} \sim L^\alpha$, we must then have

$$x \sim L e^{-L^{1+\alpha}}. \tag{11}$$

Going to real time, we instead (but equivalently) solve for $P(\downarrow)$, obtaining

$$P(\downarrow) = \frac{x^2}{x^2+\epsilon^2} \sin(t\sqrt{\epsilon^2+x^2}). \tag{12}$$

Here the oscillatory behavior clearly differs from what one would obtain in an infinite many-body system, where the initial state decays into many other states and no periodicity is expected for a thermalizing system in the thermodynamic limit. Nevertheless, one can define a rate of depletion of the initial state as the maximum $P(\downarrow)$ divided by the time taken to reach this maximum. This gives the rate (for small x/ϵ) $v = 2x^2/(\pi\epsilon)$, which, with Eq. (11) and $\epsilon \sim L$, becomes

$$v \sim L e^{-2L^{1+\alpha}}. \tag{13}$$

While the approximation of the evolution of the quantum many-body state by just a two-level system, where the two levels represent entire sectors of states (blocks in the Hamiltonian matrix), cannot be expected to be quantitatively accurate, the above simple calculation nevertheless illustrates how the imaginary-time behavior can qualitatively differ from the corresponding real-time dynamics. The exponential decay rate obtained above is most likely correct, though details such as the power α in Eq. (13) may not necessarily be accurate. It would be interesting to investigate this issue further by considering more sophisticated models with more than two states.

V. RESULTS AT THE CRITICAL POINT

Our studies of the lifetime of the winding number in the preceding sections, and the associated convergence of excited energies with system size to values consistent with the domain-wall energy per unit length, show unambiguously that the winding number is an emergent conserved quantity in the VB solid state. This in itself is perhaps not surprising, but our calculations have demonstrated the nature of the mechanism causing the winding transitions (topological fluctuations) and quantified the lifetime. An important question now is how the mechanism of winding number decay evolves as one approaches a critical point at which the VB solid order vanishes. Such a critical point can be reached in the $J - Q$ model. In the present variant with six-spin Q interaction (5) the critical value of the ratio $q = Q/(J + Q)$ is $q_c \approx 0.600$ [14].

In the theory of deconfined quantum-criticality [49], there are two relevant diverging length scales upon approaching the critical point at $q = q_c$. In addition to the standard correlation length $\xi \sim (q - q_c)^{-\nu}$, which can be defined, e.g., using the distance dependence of spin-spin or VB-VB correlations, there is a larger length scale ξ_{VB} characterizing the thickness of domain walls inside the VB solid, with $\xi_{VB} \sim (q - q_c)^{-\nu'}$ and $\nu' > \nu$ [46]. The presence of two intrinsic physical length scales in the system makes the finite-size scaling of κ very interesting, with dramatic crossovers predicted [49]. Studying κ in detail upon approaching the critical point within the $J - Q$ model is an interesting problem, which, however, is beyond the scope of the present study. We here just consider the winding number conservation and associated critical domain-wall energy as a function of the system size at the critical point. Critical domain walls have previously been studied in the classical dimer model as well as in spin-liquid wave functions defined using short VBs [50,51]. In those cases the winding number is conserved by construction.

Figure 8 shows the excitation energy (critical domain-wall energy) per unit length at $q = 0.6$, which is within error bars of the best known value of q_c for this model [14]. PQMC results for $w_x = 1$, computed in the manner discussed in Sec. III, are shown versus $1/L$ for three different cases of $\beta(L) = aL$. For reference, results deep inside the VB solid phase ($q = 1$) are also shown here. They converge to a nonzero constant as $L \to \infty$, with two choises of $\beta(L)$ seen to produce the same result. At q_c, going from $\beta = L/8$ to $L/4$, we can see a clear decrease in the energy, while upon further reducing the temperature to $\beta = 3L/8$ there are no significant changes for any L within the error bars (which now are large for large systems, making calculations at still higher β prohibitively expensive). The results shown were obtained with an initial state of the type in Fig. 1(b), but converged results from the type-(c) state are the same within error bars.

Interestingly, a very good power-law behavior is seen at q_c, $\kappa \sim L^{-b}$ with $b \approx 1.8$, which corresponds to the (quasi-) eigenenergy $E_0(w_x = 1) \sim L^{1-b} \approx L^{-0.8}$. The lowest singlet energy in the $J - Q$ model at q_c scales as $1/L$ [52], as expected for a critical point with dynamic exponent $z = 1$. Thus, the critical domain-wall energy is only slightly above the lowest singlet (and it should be noted here again that the momentum of all the states we are computing here is 0, as in the ground state).

The domain-wall energy per unit length of a VB solid can be expressed as

$$\kappa = \frac{K}{\Lambda}, \tag{14}$$

where K is a stiffness constant describing the energy cost of a twist of the VB order parameter and Λ is the width of the region over which this twist is distributed. In the theory of deconfined quantum-criticality [49], the VB stiffness in the thermodynamic limit scales as $K \sim \xi^{-1} \sim (q - q_c)^{-\nu}$ upon approaching the critical point, while Λ must saturate at the domain-wall thickness discussed above. Thus, in systems with domain walls imposed through winding numbers, one can expect that

$$\kappa \sim \frac{1}{\xi} \frac{1}{\xi_{\text{VB}}} \sim (q - q_c)^{\nu' + \nu}. \tag{15}$$

In standard finite-size scaling procedures at a critical point [53], to relate the behavior of a quantity in the thermodynamic limit as a critical point is approached to the behavior as a function of the system size exactly at the critical point, one simply replaces the correlation length by the system length L. In the present case, we can argue that it is ξ_{VB} that should be replaced by L, since this length scale is the one reaching L first when q_c is approached for finite L. We then obtain

$$\kappa(q_c) \sim L^{-(1+\nu/\nu')}, \tag{16}$$

and, therefore, with the exponent b defined in the analysis of our results above (shown in Fig. 8) we have $b = 1 + \nu/\nu'$. Thus, we have extracted a rather precise estimate of the exponent ratio $\nu/\nu' \approx 0.80 \pm 0.01$, where the error bar is one standard deviation of the slope of the fitted line in Fig. 8 (and we estimate that the error due to very small deviations of $q =$
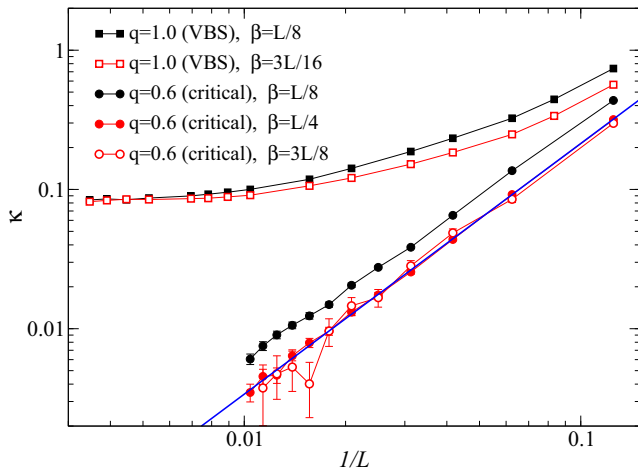

FIG. 8. (Color online) VB domain-wall energy per unit length as a function of the inverse system size graphed on a log-log scale. In the case of the strongly ordered VB solid ($q = 1$), the energy computed with two different inverse temperatures $\beta(L)$ converges to the same nonzero value as $L \to \infty$, while at the critical point ($q = 0.6 \approx q_c$) convergence of the energy for all L with increasing β is demonstrated (the same also holds true at $q = 1$ if still larger β is used). The converged energy decays as a power-law form $\sim L^{-b}$. The fitted line shown here has slope $b = 1.80 \pm 0.01$.
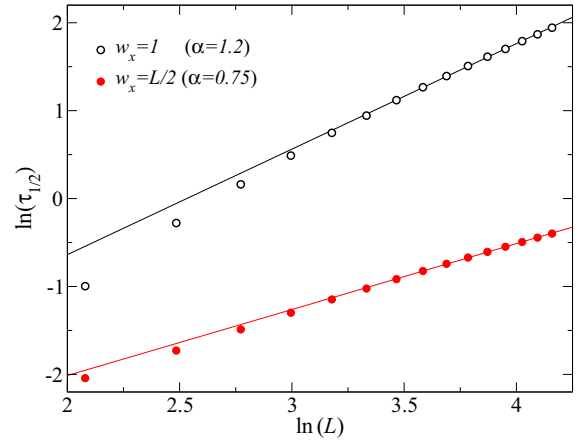

FIG. 9. (Color online) Size dependence of the imaginary-time lifetime at q_c of states with winding numbers $w_x = 1$ and $w_x = L/2$, using initial states of the type in Fig. 4(b) and its $w_x > 1$ generalization. The lines drawn through the large-L points have slopes $\alpha = 1.2$ and $\alpha = 0.75$ for $w_x = 1$ and $w_x = L/2$, respectively.

0.6 from the true q_c is smaller than the quoted statistical error). The only other estimate of this exponent ratio that we are aware of is $\nu'/\nu = 1.20 \pm 0.05$, or $\nu/\nu' = 0.83 \pm 0.04$, from an analysis of the emergent U(1) symmetry of the VB order parameter [14]. It is gratifying that these two estimates obtained in completely different ways are fully consistent with each other.

Now consider the lifetime in imaginary time, calculated as in Sec. III. Figure 9 shows results for $w_x = 1$ as well as the extreme case of $w_x = L/2$. We find $\tau_{1/2} \sim L^{1.2}$ for $w_x = 1$ and $\tau_{1/2} \sim L^{0.75}$ for $w_x = L/2$ (with error bars on the exponents of about 10%). In the effective real-time model, with the critical domain-wall energy scaling as $E_W - E_{W-1} \sim \kappa L \sim L^{1-b}$, the form (13) of the decay rate derived in the VBS (where the energy difference scales as L) becomes

$$v \sim L e^{-2L^{1-b+\alpha}}. \tag{17}$$

At $w_x = 1$ the exponent $1 - b + \alpha$ remains positive with the values of α and b obtained above, and, thus, the transition rate out of the original w_x sector in real time is exponentially small. It is interesting that for $w_x = L/2$ our results suggest $1 - b + \alpha \approx 0$ (within estimated error bars) and if this exponent indeed vanishes, and if the two-state model is to be taken seriously (which perhaps is asking too much of it in this extreme case), then the high-winding states would actually have a shorter than exponentially long lifetime at the critical point.

Going to coupling ratio $q < q_c$, entering the antiferromagnetic state of the $J - Q$ model, the winding number sectors should become completely unstable. Indeed, here the energy above the ground state computed with different $\beta = aL$ quickly decays to 0 and, unlike the results at q_c in Fig. 8, it is not possible to discern any converged functional form.

VI. SUMMARY AND DISCUSSION

We have demonstrated a mechanism of decay of domain walls in a VB solid state of a quantum spin system through fluctuations of the topological winding number which

effectively counts the number of domain walls in a system. The mechanism requires the wave function to contain VBs of length proportional to the system size, which is explicitly excluded in an effective description of VB solids with a QDM. The domain walls become stable in the thermodynamic limit, or, in other words, the winding number is an emergent conserved quantum number. The lifetime in imaginary time scales as a power of the system size and we have argued, based on a simple two-state model for two winding sectors, that this translates into an exponentially small transition rate out of an initial winding-number sector in real time.

At a critical point separating the VB solid and an antiferromagnetic ground state (the putative deconfined quantum-critical point [49]), we have also found stable winding numbers in the thermodynamic limit and a power-law decay of the excitation energy with the system size. The energy decay exponent contains information on the spectrum of the effective $U(1)$ gauge-field model describing this phase transition, and our quantitative results from the power-law scaling, along with exponents obtained previously for other quantities [14], lend support to the CP^1 field theory of deconfined quantum-criticality [49]. It would be interesting to study in detail the domain-wall energy in the whole range of states between the maximally ordered VB solid and the critical point to make further quantitative comparisons with the theory.

It would be interesting to investigate the consequences of long VBs in spin liquid phases as well (noting that the critical point we have consider corresponds to an algebraic spin liquid at an isolated point). To our knowledge, the expected quasidegenerate topological multiplet has never been observed in SU(2)-invariant Z_2 spin-liquid candidate Hamiltonians [54–57] (which are amenable to VB descriptions and whose topological numbers should be similar to the even-odd winding discussed in Ref. [19]). This could be due to the splitting being relatively large, perhaps still exponentially small but with a large prefactor, or there could be some crossover from a different form when the system size is still relatively small and the effects of longer VBs could be significant. It should be noted here that, because of the overcompleteness of the VB basis, to fix the winding number of an initial state it must overlap with states also outside the subspace of the topological multiplet of a gapped spin liquid. Some of these states may also have an enhanced fraction of long VBs, as we found here in the transitional states out of simple short-bond domain-wall states. Spin liquids in frustrated spin models cannot be investigated with the PQMC methods we have used here, due to sign problems, but it may be possible to study this issue with exact diagonalization techniques based on VBs [58], though the limitation in system size may make it difficult to clearly observe the effects of long bonds.

[1] A. Y. Kitaev, in *Proceedings of the 3rd International Conference of Quantum Communication and Measurement*, edited by O. Hirota, A. S. Holevo, and C. M. Caves (Plenum, New York, 1997).

[2] A. Y. Kitaev, Ann. Phys. **303**, 2 (2003).

[3] A. G. Fowler, M. Mariantoni, J. M. Martinis, and A. N. Cleland, Phys. Rev. A **86**, 032324 (2012).

[4] R. Barends *et al.*, Nature **508**, 500 (2014).

[5] G. Misguich, V. Pasquier, F. Mila, and C. Lhuillier, Phys. Rev. B **71**, 184424 (2005).

[6] A. F. Albuquerque, H. G. Katzgraber, M. Troyer, and G. Blatter, Phys. Rev. B **78**, 014503 (2008).

[7] E. Fradkin, D. A. Huse, R. Moessner, V. Oganesyan, and S. L. Sondhi, Phys. Rev. B **69**, 224415 (2004).

[8] S. Papanikolaou, K. S. Raman, and E. Fradkin, Phys. Rev. B **75**, 094406 (2007).

[9] P. W. Anderson, Science **235**, 1196 (1987).

[10] N. Read and S. Sachdev, Phys. Rev. Lett. **66**, 1773 (1991).

[11] X.-G. Wen, Phys. Rev. B **44**, 2664 (1991).

[12] X.-G. Wen, Phys. Rev. B **65**, 165113 (2002).

[13] A. W. Sandvik, Phys. Rev. Lett. **98**, 227202 (2007).

[14] J. Lou, A. W. Sandvik, and N. Kawashima, Phys. Rev. B **80**, 180414(R) (2009).

[15] L. Hulthén, Ark. Mat. Astr. Fys. **26**, 1 (1938).

[16] S. Liang, B. Doucot, and P. W. Anderson, Phys. Rev. Lett. **61**, 365 (1988).

[17] B. Sutherland, Phys. Rev. B **37**, 3786(R) (1988)

[18] K. Beach and A. W. Sandvik, Nucl. Phys. B **750**, 142 (2006).

[19] N. E. Bonesteel, Phys. Rev. B **40**, 8954 (1989).

[20] A. W. Sandvik, Phys. Rev. Lett. **95**, 207203 (2005).

[21] A. W. Sandvik and H. G. Evertz, Phys. Rev. B **82**, 024407 (2010).

[22] S. A. Kivelson, D. S. Rokhsar, and J. P. Sethna, Phys. Rev. B **35**, 8865(R) (1987).

[23] D. S. Rokhsar and S. A. Kivelson, Phys. Rev. Lett. **61**, 2376 (1988).

[24] R. Moessner, S. L. Sondhi, and E. Fradkin, Phys. Rev. B **65**, 024504 (2001).

[25] A. W. Sandvik and R. Moessner, Phys. Rev. B **73**, 144504 (2006).

[26] H. Yao and S. A. Kivelson, Phys. Rev. Lett. **108**, 247206 (2012).

[27] S. Sachdev, Phys. Rev. B **40**, 5204 (1989).

[28] G. Misguich, D. Serban, and V. Pasquier, Phys. Rev. B **67**, 214413 (2003).

[29] F. Vernay, A. Ralko, F. Becca, and F. Mila, Phys. Rev. B **74**, 054402 (2006).

[30] D. Poilblanc, M. Mambrini, and D. Schwandt, Phys. Rev. B **81**, 180402(R) (2010).

[31] A. Ralko, M. Mambrini, and D. Poilblanc, Phys. Rev. B **80**, 184427 (2009).

[32] A. F. Albuquerque, D. Schwandt, B. Hetényi, S. Capponi, M. Mambrini, and A. M. Läuchli, Phys. Rev. B **84**, 024406 (2011).

[33] N. Read and S. Sachdev, Phys. Rev. Lett. **62**, 1694 (1989).

[34] E. Dagotto and A. Moreo, Phys. Rev. Lett. **63**, 2148 (1989).

[35] M. P. Gelfand, R. R. P. Singh, and D. A. Huse, Phys. Rev. B **40**, 10801 (1989).

[36] H. J. Schulz, T. Ziman, and D. Poilblanc, J. de Physique. I **6**, 675 (1996).

[37] V. N. Kotov, J. Oitmaa, O. P. Sushkov, and Z. Weihong, Phys. Rev. B **60**, 14613 (1999).

[38] A. Läuchli, J. C. Domenge, C. Lhuillier, P. Sindzingre, and M. Troyer, Phys. Rev. Lett. **95**, 137206 (2005).

[39] A. Sen and A. W. Sandvik, Phys. Rev. B **82**, 174428 (2010).

[40] A. W. Sandvik, Phys. Rev. B **85**, 134407 (2012).

[41] The method is a simple generalization of the scheme developed in Ref. [21], with Taylor-expanded exponential as in the stochastic series expansion method [42,43], instead of projecting with a fixed power of H.

[42] A. W. Sandvik, Phys. Rev. B **59**, R14157 (1999).

[43] A. W. Sandvik, AIP Conf. Proc. **1297**, 135 (2010).

[44] H. Shao, W. Guo, and A. W. Sandvik, arXiv:1501.00237.

[45] In Ref. [44] the energy was computed in a slightly different way, using the form $\langle N|HH^m|\Psi_0(w_x)\rangle/\langle N|H^m|\Psi_0(w_x)\rangle$, where $|N\rangle$ refers to one of the fully ordered z-component Néel states. This is not a variational estimator but nevertheless it approaches the exact ground-state energy when $m \to \infty$ [20]. When using this estimator in fixed winding-number sectors, by following the VB evolution involved in $H^m|\Psi_0(w_x)\rangle$, we find small deviations from the results reported in this paper (though still reasonable agreement with the expected domain-wall energies, as reported in Ref. [44]). These differences should originate from the fact that $|N\rangle$ is not a state with a fixed winding number, and, thus, the energy estimator to some extent mixes in states with winding number different from the starting w_x. The method used in the present paper does not have this problem, because an expectation value between two states with well-defined W is computed.

[46] M. Levin and T. Senthil, Phys. Rev. B **70**, 220403(R) (2004).

[47] C.-W. Liu, A. Polkovnikov, and A. W. Sandvik, Phys. Rev. B **87**, 174302 (2013).

[48] C. De Grandi, A. Polkovnikov, and A. W. Sandvik, Phys. Rev. B **84**, 224303 (2011).

[49] T. Senthil, L. Balents, S. Sachdev, A. Vishwanath, and M. P. A. Fisher, Phys. Rev. B **70**, 144407 (2004).

[50] Y. Tang, A. W. Sandvik, and C. L. Henley, Phys. Rev. B **84**, 174427 (2011).

[51] A. F. Albuquerque and F. Alet, Phys. Rev. B **82**, 180408 (2010).

[52] A. Sen, H. Suwa, and A. W. Sandvik (unpublished).

[53] M. N. Barber, in *Phase Transitions and Critical Phenomena*, Vol. 8, edited by C. Domb and J. Lebowitz (Academic Press, London, 1983).

[54] S. Yan, D. A. Huse, and S. R. White, Science **332**, 1173 (2011).

[55] A. M. Läuchli, J. Sudan, and E. S. Sørensen, Phys. Rev. B **83**, 212401 (2011).

[56] S. Depenbrock, I. P. McCulloch, and U. Schollwöck, Phys. Rev. Lett. **109**, 067201 (2012).

[57] I. Rousochatzakis, Y. Wan, O. Tchernyshyov, and F. Mila, Phys. Rev. B **90**, 100406(R) (2014).

[58] M. Mambrini, A. Läuchli, D. Poilblanc, and F. Mila, Phys. Rev. B **74**, 144422 (2006).